

Enhancing Local Feature Learning Using Diffusion for 3D Point Cloud Understanding

Haoyi Xiu^{1,2}, Xin Liu¹, Weimin Wang^{2,3}, Kyoung-Sook Kim², Takayuki Shinohara⁴, Qiong Chang⁵, and Masashi Matsuoka¹

¹ Department of Architecture and Building Engineering, Tokyo Institute of Technology, Tokyo, Japan

² Artificial Intelligence Research Center, AIST, Tokyo, Japan

³ DUT-RU International School of Information Science and Engineering, Dalian University of Technology, Dalian, China

⁴ Innovation Technology Office Research Center, PASCO Corporation, Tokyo, Japan

⁵ Department of Computer Science, Tokyo Institute of Technology, Tokyo, Japan

Abstract. Learning point clouds is challenging due to the lack of connectivity information, i.e., edges. Although existing edge-aware methods can improve the performance by modeling edges, how edges contribute to the improvement is unclear. In this study, we propose a method that automatically learns to enhance/suppress edges while keeping the its working mechanism clear. First, we theoretically figure out how edge enhancement/suppression works. Second, we experimentally verify the edge enhancement/suppression behavior. Third, we empirically show that this behavior improves the performance. In general, we observe that the proposed method achieves competitive performance in point cloud classification and segmentation tasks.

Keywords: edge enhancement; edge suppression; edge awareness; diffusion; point clouds

1 Introduction

A 3D point cloud is the most basic shape representation in which the scanned surface is represented as a set of points in the 3D space. With the advent of cost-effective sensors, an increasing number of large-scale point cloud datasets have been released to researchers, facilitating deep learning-based point cloud understanding. Typical applications of such research include autonomous driving [9,31] and remote sensing [59,36].

A point cloud is naturally unordered and unstructured, hindering the application of convolutional neural networks (CNNs) that are suited for processing regular grid data. Therefore, many prior studies have focused on applying CNNs by projecting point clouds to regular grids [18,39,28,58]. However, there is information loss incurred by the projection and these approaches are sub-optimal. To remedy this issue, PointNet applies shared multi-layer perceptrons (MLPs) and symmetric functions to raw 3D points, consuming point cloud in a

lossless manner [32]. PointNet++ subsequently applies PointNets to local subsets of points, obtaining CNN-like translation invariance [33]. Recently, various convolution methods that operate directly on raw point clouds have been developed [23,47,41,24]. Despite these efforts, learning point cloud data remains challenging due to the difficulty in inferring the underlying continuous surface from discrete point samples.

In recent years, people find that exploring the connectivity information between points (i.e., edges) is beneficial for 3D point cloud understanding and developed edge-aware approaches. For instance, researchers treat edges as additional contextual features [44,25,48] or spatial weights [43,55,56] that describe local geometrical structures and incorporate them into their models. Although incorporating edge information successfully improves the model performance, the underlying mechanism of *how* edges contribute to the improvement is not clear. Moreover, some researchers explicitly supervise the model with edge information [17,16,53]. However, these methods require per-point and clean ground truth labels (possibly with additional annotations), which are costly and not always available in practice.

In this study, we go beyond edge awareness, and propose the diffusion unit (DU) that performs automatic edge enhancement/suppression learning without additional supervision. Built on the nonlinear diffusion theory [30,45], DU adaptively enhances task-beneficial edges and suppress irrelevant ones so as to improve the performance. In contrast to existing works, the mechanism of edge enhancement/suppression is interpretable in terms of theoretical analysis and experimental verification. Specifically, 1) We theoretically figure out which component of our method is responsible for edge enhancement/suppression and how it works; 2) We experimentally observe and verify the edge enhancement/suppression behavior; 3) We empirically demonstrate that this behavior contributes to the performance improvement.

DU is generally applicable, as it can be seamlessly integrated with a convolution operator as a basic building block of deep neural networks. Particularly, we resort to KPConv [41] as the default convolution operator owing to its superiority in point cloud processing. Further, to better fitting to DU, we develop a lightweight variant of KPConv, namely KPConv-l, which provides decent performance while drastically reducing the number of parameters.

Stacking KPConv-l and DU as a basic building block, we construct DU-Nets to tackle point cloud understanding tasks. Extensive experiments across several standard benchmarks demonstrate its effectiveness. In particular, we achieve the state-of-the-art performance in point cloud classification and comparative performance in part segmentation and scene segmentation.

Our main contributions are summarized as follows:

- We propose DU that performs automatic edge enhancement and suppression learning so as to improve the performance.
- We theoretically analyze and experimentally verify the edge enhancement and suppression behavior of DU.

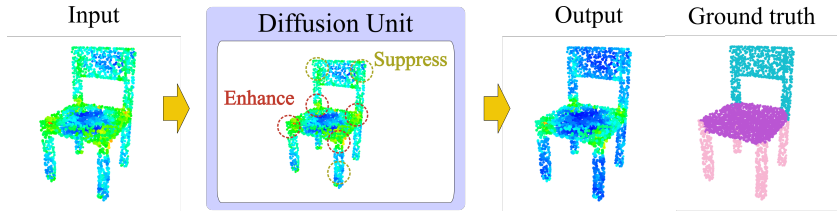


Fig. 1. Overview of the diffusion unit (DU). DU automatically learns to enhance task-beneficial edges or suppress irrelevant edges so as to improve the performance.

- We propose a lightweight version of KPConv, KPConv-l, which drastically reduces the number of parameters without compromising the performance.
- We design DU-Nets by stacking KPConv-l and DU as the basic building block and achieve the state-of-the-art performance in point cloud classification and comparative performance in part segmentation and scene segmentation tasks.

2 Related Work

2.1 Deep learning for 3D Point Clouds

Projection-based methods Projection-based methods project point clouds to regular grids (e.g., 2D planes [18,39,11] and 3D voxels [28,58,13,7]) to make matured regular convolution applicable to point clouds. However, they lose fine-grained details through projections.

MLP-based methods Pioneered by PointNet [32], MLP-based methods prevent information loss by operating directly on the raw points. PointNet relies on shared MLPs and symmetric functions; both operations are permutation-invariant, and thus the irregularity of point clouds is well-resolved. Subsequently, PointNet++ [33] have made major steps toward the convolution-like operation by applying shared MLPs to local subsets of points [54,21].

Convolution-based methods A variety of point convolutions have been realized by defining convolution operations on unstructured point clouds. Some studies construct regular kernels/grids on which the points are projected, thus enabling the faithful extension of the standard convolution [41,27]; the others dynamically generate convolution filters based on positional features [23,47]. Though being effective, convolution-based methods do not explicitly model local structures which potentially can provide more accurate representations of the underlying surface.

Edge-aware methods Edge-aware methods explicitly integrate edge information into the network design. Pioneered by EdgeConv [44], these methods perform convolution on the edge embedding to better model the local geometric structure. The idea of EdgeConv is adopted in numerous subsequent works (e.g.,

[38,22,25,50,48]). Although performance improves, it is difficult to analyze rigorously how it is improved. Furthermore, local edge features are simply fused with global ones by MLPs, which may be suboptimal since they are significantly distinct features. On the other hand, some methods regard edge information as a similarity measure, representing the semantic distance. In [43], such a similarity is used for describing connectivity among neighboring points; consequently, the information exchange is guided by edge information. Such an operation is often coupled with the attention mechanism [55,56,49], which converts edge into normalized spatial weights. However, the forced conversion may lose rich structural information (e.g., smoothness) contained in the edges. Another type of approach explicitly guides the network by edge-related supervision. Specifically, networks are taught to maintain spatial consistency [17], perform edge detection and other tasks jointly [16] or be aware of the location of edges [53]. Such methods involve dedicated loss functions or models, and often require clean and per-point ground truth, thereby making their practical applications challenging.

In contrast to the aforementioned edge-aware methods, the proposed DU goes beyond edge awareness by automatically learning to enhance task-beneficial edges and suppress irrelevant ones, thereby improving the performance. Furthermore, compared with existing edge-aware methods, DU offers significantly better interpretability through both theoretical and qualitative analysis.

2.2 Diffusion

In essence, diffusion methods, which are motivated by the diffusion equation, model the smoothing of data (e.g., images) as diffusion processes. The core of the diffusion methods is the diffusivity [30,4], which is often defined as a function of edge. As a result, diffusion methods remove small edges (small edges) while preserving significant edges [30], making them attractive to various applications. Therefore, such techniques are extensively studied in image processing [30,45,46,5] and later by other communities (e.g., computer graphics [10,8,3]). In the context of deep learning, although several works model the global information propagation [2,57,6] or the probabilistic point cloud generation [26] as diffusion processes, extending the diffusion equation for adaptive edge enhancement/suppression for 3D point cloud understanding, which we exclusively cope with in this study, remain unexplored.

3 Diffusion Unit

In this part, we first provide a brief background about the diffusion equation to build intuition. Next, we present the (continuous) definition of DU. Then, we perform a theoretical analysis to reveal the underlying mechanism of edge enhancement/suppression learning. Subsequently, we provide the discretization scheme that enables an efficient implementation of DU on modern machines. To enable a seamless integration of DUs to modern CNN-based frameworks, we explain how DUs can be integrated with KPConv-l. Lastly, we describe the network architectures used for various analyses and experiments in this study.

3.1 Preliminary

The diffusion equation describes the movement of diffusive substances from regions of higher concentration to lower concentration without creating or destroying mass [45]. For instance, when hot water is poured into cold water, heat diffuses until the temperature of the water becomes the same everywhere. Let $u(p, t)$ denote the concentration at the position p and time t . The amount of substances that flow through per unit area per unit time (the flux) is described by Fick’s law:

$$s = -g \cdot \nabla u, \quad (1)$$

where ∇ denotes the gradient operator and g denotes the diffusivity. The fact that diffusion processes do not create or destroy mass is expressed by the continuity equation:

$$\partial_t u = -\text{div}(s). \quad (2)$$

The continuity equation indicates that the change of concentration is caused only by the flux, which is measured by the divergence operator (div). Finally, the diffusion process is described by combining the above two equations:

$$\partial_t u = \text{div}(g \cdot \nabla u) \quad t \geq 0, \quad (3)$$

with the initial condition $u(p, 0) = u_0(p)$ and the boundary condition as appropriate.

3.2 Definition of Diffusion Unit

Inspired by the diffusion equation, we propose diffusion unit (DU) that facilitates the edge enhancement learning for 3D point clouds. Suppose a continuous spatial-temporal multi-channel point cloud $\mathbf{u} = \mathbf{u}(\mathbf{p}, t) = (u_1(\mathbf{p}, t), u_2(\mathbf{p}, t), \dots, u_d(\mathbf{p}, t))$, where d is the number of channels, t is time, \mathbf{p} denotes the position vector, and the initial condition is $\mathbf{u}(\mathbf{p}, 0) = \mathbf{h}$. DU is defined as:

$$\partial_t \mathbf{u} = \text{div}(\phi(\nabla \mathbf{u})), \quad t \geq 0, \quad (4)$$

where $\partial_t \mathbf{u} \in \mathbb{R}^d$ is the output of DU at time t , $\nabla \mathbf{u}$ encodes channel-wise spatial gradient. Note that the choice of diffusivity g in Eq. (3) has a significant impact on performance. Finding the appropriate g often requires domain knowledge and involves numerous trials and errors [4]. In our definition, we replace the handcrafted g with a *trainable filter* $\phi: \mathbb{R}^d \rightarrow \mathbb{R}^d$ so that the diffusivity function can be learned w.r.t data and task. In practice, we use **1D-Conv** to implement ϕ to maintain the local behavior. Note that ϕ is a multi-channel filter that mixes information in all channels, since each channel may contain a fragment of information with certain degrees of noise.

3.3 Edge Enhancement/Suppression Learning

Now we explain how DU performs edge enhancement/suppression learning.

For simplicity, we consider a step edge convolved by a Gaussian. Ideally, such a structure can be detected by the spatial gradient $\nabla \mathbf{u}$. Without loss of generality, we assume that the edge is aligned with x axis ($\mathbf{u}_y = \mathbf{u}_z = \mathbf{0}$). The profile of the step edge and its derivatives are illustrated in Fig. 2. Now we focus on a single output channel i for brevity.

In this context, Eq. (4) can be simplified as

$$(\partial_t \mathbf{u})_i = \frac{\partial}{\partial x} (\phi_i(\mathbf{u}_x)) = \nabla \phi_i \cdot \mathbf{u}_{xx} \quad (5)$$

$$= \sum_{j=1}^d (\phi'_i)_j \cdot (\mathbf{u}_{xx})_j, \quad i = 1, 2, \dots, d. \quad (6)$$

We are interested in the evolution of the edge over time, i.e., how \mathbf{u}_x changes during applications of DU. We can derive that:

$$(\partial_t \mathbf{u}_x)_i = \left(\frac{\partial}{\partial t} \frac{\partial \mathbf{u}}{\partial x} \right)_i = \frac{\partial}{\partial x} \left(\frac{\partial \mathbf{u}}{\partial t} \right)_i \quad (7)$$

$$= \frac{\partial}{\partial x} \left(\sum_{j=1}^d (\phi'_i)_j \cdot (\mathbf{u}_{xx})_j \right) \quad (8)$$

$$= \sum_{j=1}^d (\phi''_i)_j \cdot (\mathbf{u}_{xx})_j^2 + (\phi'_i)_j \cdot (\mathbf{u}_{xxx})_j. \quad (9)$$

As shown in Fig. 2, at the inflection point $\mathbf{u}_{xx} = 0$ and $\mathbf{u}_{xxx} < 0$. Therefore, the contribution of a particular input channel j to the output channel i (the sign of Eq. (9)) is determined by the sign of $(\phi'_i)_j$. Specifically, channel j has a positive impact if $(\phi'_i)_j < 0$, whereas it has a negative impact if $(\phi'_i)_j > 0$.

As a result, enhancing ($(\partial_t \mathbf{u}_x)_i > 0$) or suppressing ($(\partial_t \mathbf{u}_x)_i < 0$) the edge can be adaptively learned by the filter ϕ , by collectively using fragmentary information in all channels.

3.4 Discretization

To deal with discrete point clouds, discretization of Eq. (4) is necessary. Let $\mathbf{u}_s, \mathbf{u}_n \in \mathbb{R}^d$ denote the feature of the center point and its spatial neighbors, respectively. Let $n \in \mathcal{N}_s$ represents n -th neighbor of the center point. First, we adopt the explicit scheme for time discretization and have:

$$\partial_t \mathbf{u}_s \approx \mathbf{u}_s^{t+1} - \mathbf{u}_s^t. \quad (10)$$

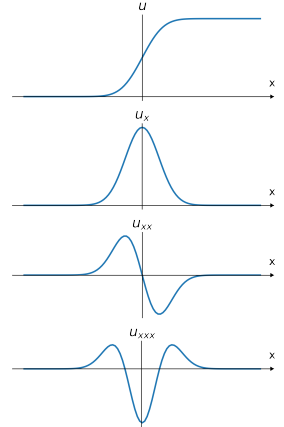


Fig. 2. Profiles of the smoothed step edge and its derivatives.

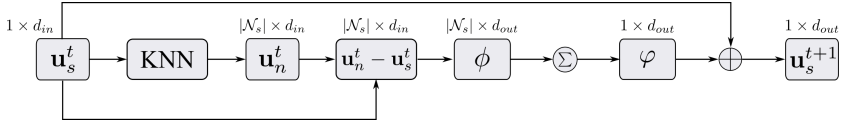


Fig. 3. The computation flow of DU. The input dimension is the same as the output dimension ($d_{in} = d_{out}$). \oplus indicates the element-wise addition.

Second, we discretize the space using the finite difference and have:

$$\operatorname{div}(\phi(\nabla \mathbf{u})) \approx \frac{1}{|\mathcal{N}_s|} \sum_{n \in \mathcal{N}_s} \phi(\mathbf{u}_n^t - \mathbf{u}_s^t), \quad (11)$$

where $|\mathcal{N}_s|$ represents the number of neighbors. Combining Eqs. (4), (10), (11), we have

$$\mathbf{u}_s^{t+1} = \mathbf{u}_s^t + \left(\frac{1}{|\mathcal{N}_s|} \sum_{n \in \mathcal{N}_s} \phi(\mathbf{u}_n^t - \mathbf{u}_s^t) \right). \quad (12)$$

Moreover, we incorporate Batch Normalization and ReLU activation function $\varphi = \text{BatchNorm} \cdot \text{ReLU} : \mathbb{R}^d \rightarrow \mathbb{R}^d$ into the second term on the right-hand side of Eq. (12) to facilitate training and encourage sparsity. Finally, the discretized DU is defined as:

$$\mathbf{u}_s^{t+1} = \mathbf{u}_s^t + \varphi \left(\frac{1}{|\mathcal{N}_s|} \sum_{n \in \mathcal{N}_s} \phi(\mathbf{u}_n^t - \mathbf{u}_s^t) \right). \quad (13)$$

Note that the neural network functions ϕ and φ work together and are responsible for the learning of enhancing or suppressing edges (we provide qualitative analysis on the behavior of ϕ and φ in Sec. 4.1). The above definition can be efficiently computed and easily parallelized, fitting to modern GPU-empowered deep learning frameworks. The computation flow of DU is shown in Fig. 3.

3.5 Integrating with a Lightweight Point Convolution

DU can be integrated with a convolution operator to build a basic building block of a deep neural network. In particular, we choose KPConv [41] as the default convolution operator, owing to its superiority in point cloud processing. However, it suffers from high memory consumption, hindering its application to voluminous data. Therefore, we further develop a lightweight version of KPConv (KPConv-l) to achieve decent performance while drastically reducing the model parameters.

Lightweight KPConv KPConv adapts the standard convolution for regular data to the point cloud setting by constructing artificial convolution kernels, to which the input points are projected. However, the resulting convolution is parameter-consuming, which limits its applications to voluminous point clouds.

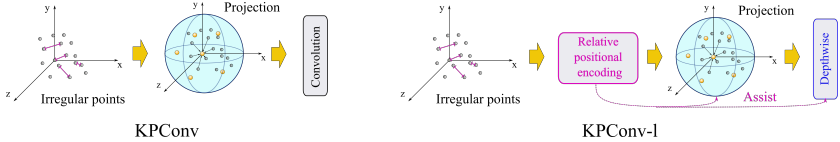


Fig. 4. Differences between KPCConv [41] and KPCConv-l. KPCConv-l reduces the complexity by replacing standard convolution with the depthwise one. Further, to assist the capacity-limited depthwise convolution to handle irregular spacing of points, relative positional encoding is applied to the raw input points.

Specifically, let l denote the number of neighbors involved in the convolution. Further, let d_{in}, d_{out} denote the dimensions of input channel and output channel, respectively. The standard convolution requires $l \times d_{in} \times d_{out}$ parameters, which leads to excessive memory consumption. To remedy this issue, we borrow the idea from prevalent depthwise separable convolution (DSC) [37] to simplify the KPCConv into depthwise KPCConv (with a depth multiplier [15]). As a result, the number of parameters is reduced to $l \times d_{out}$, thereby significantly reducing the memory consumption.

A potential concern is that, unlike data that have regular spacing between elements (e.g., image), point clouds typically have irregular spacing, which poses a great challenge to capacity-limited depthwise KPCConv. Therefore, we apply relative positional encoding on the *raw* input points to assist depthwise KPCConv to learn the irregular spacing. Specifically, relative positional encoding transforms the position-concatenated point features by an MLP such that subsequent operations become position-aware. Though simple, this trick effectively reduces memory consumption without compromising the performance. The differences of KPCConv and KPCConv-l are shown in Fig. 4.

Integration Strategy In this study, we stack a KPCConv-l and a DU to obtain the feature representation. Concretely, the input is transformed by a KPCConv-l, which is followed by a DU. Popular architectures in point cloud processing typically down-sample the input in a convolution layer; therefore, attaching DU to each convolution layer facilitates the network to learn the multi-resolution edge hierarchy.

3.6 Network Architecture

In this study, we tackle point cloud classification and segmentation. We construct Diffusion Unit-Enhanced Networks (DU-Nets) by stacking KPCConv-l and DU as the basic building block. For classification, we follow multi-scale PointNet++ [33] to construct an encoder composed of four pairs of KPCConv-l and DU. Each layer downsamples the input point cloud using the furthest point sampling [33]. The global representation is obtained by applying a pooling layer to the last layer of the encoder, and is subsequently fed to the MLPs to generate the class scores. For segmentation, we adopt the same encoder as the classification model. Then, the output of the encoder is successively upsampled to the original resolution

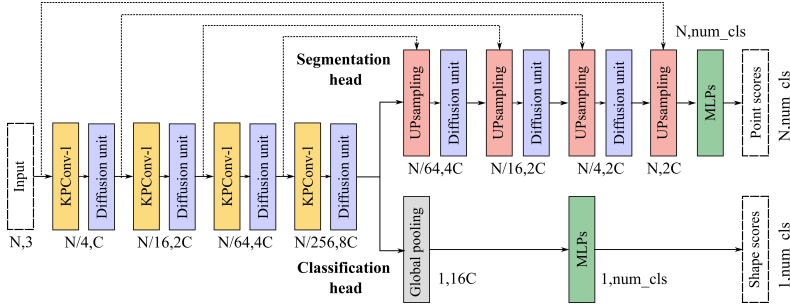


Fig. 5. The architecture of the model used in this study. N , C denote the number of input points and channels, respectively.

using 3-nearest neighbor upsampling layers. Notably, each interpolation layer is followed by a DU such that salient edges are kept sharpened. The final per-point scores are obtained by feeding the output of the decoder to a series of MLPs. In addition, U-Net [34]-like skip connections are used to assist the feature upsampling. The architecture is illustrated in Fig. 5.

4 Experiment

In this section, we conduct experiments to answer the following questions:

- Q1. Does DU really perform edge enhancement/suppression?
- Q2. How much does DU contribute to improve the performance?
- Q3. Is DU-Net better than existing deep learning models?
- Q4. Is the design of the different components of DU-Net reasonable?

To answer these questions, we use standard benchmark tests on point cloud classification, part segmentation, and scene segmentation tasks.

For classification, we use ScanObjectNN [42], which is a challenging dataset consisting of real-world 3D scans. In total, it contains 15k objects, each being labeled into one of the 15 categories.

For part segmentation, we use ShapeNet Part dataset [52], which includes 16,880 models 3D models. It includes 16 object classes and 50 object parts, each of which is annotated into two to six parts. For a fair comparison, we use the data provided by [33].

For scene segmentation, Stanford large-scale 3D indoor spaces (S3DIS) [1] is used to measure the performance. In total, it has 272 indoor environments where each point is assigned a class out of 13 classes.

4.1 Verifying the Behaviors of DU

We have theoretically analyzed that the neural network functions ϕ and φ work together and are responsible for the learning of enhancing or suppressing edges.

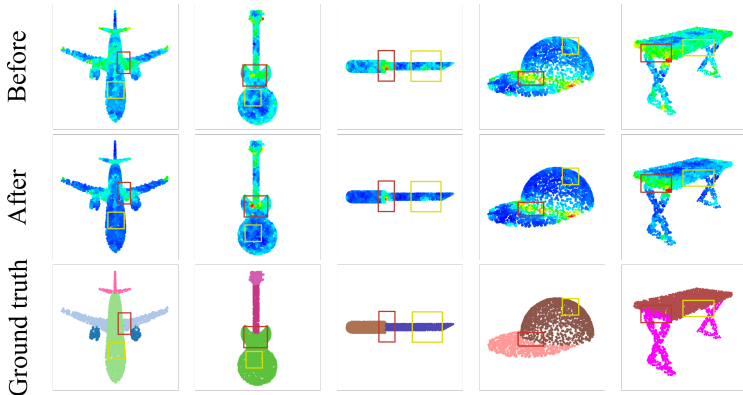


Fig. 6. Visualization of the smoothness using ShapeNet dataset (part segmentation). **Red** rectangles show the examples of enhanced part, while **yellow ones** show the suppressed part. DU successfully enhances the part boundaries while smoothing out other edges.

Here we experimentally verify the edge enhancement/suppression behaviors. Specifically, we perform qualitative analysis on *smoothness*, which reflects the effects of DU. Let $\mathbf{f} \in \mathbb{R}^d$ denote the processed features. Formally, the smoothness is defined as: $\|\sum_{n \in \mathcal{N}_s} \mathbf{f}_n - \mathbf{f}_s\|$, which essentially summarizes how the center point is different from its neighbors. As such, we compute the smoothness before and after applying DU to analyze the behavior of DU.

Fig.6 and 7 show several examples from ShapeNet and S3DIS datasets on which our part and scene segmentation models are trained. For each example, smoothness distributions before and after DU are extracted and compared. We find that 1) DU successfully enhances the part boundaries and smooths out other intra-region edges in the part segmentation task; 2) DU manages to enhance inter-category edges while suppressing intra-category ones, making object boundaries more salient. Therefore, the task-beneficial edge enhancement/suppression behavior of DU can be verified.

4.2 Point Cloud Classification

We use the most difficult set of the dataset and adopt the official train-test split [42]. The performance is measured by the overall accuracy (OA). We use Adam [20] optimizer with an initial learning rate of 0.001. The input is augmented by random rotation, scaling, and translation. Only the 3D coordinates are used as input features. Furthermore, we vary the input number of points (1,024 and 2,048) to investigate the impact of the increased training data.

The result is listed in Table 1. The DU-Nets outperform the previous leading methods by significant margins under both experimental settings, which verifies their effectiveness on the classification task. We observe that increasing the number of input points significantly improves the performance. We conjecture

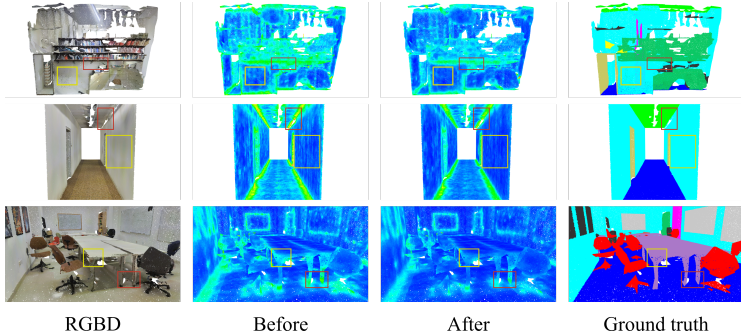


Fig. 7. Visualization of the smoothness using S3DIS dataset (scene segmentation). Red rectangles show the examples of enhanced part, while yellow ones show the suppressed part. DU manages to enhance the task-related edges while suppressing irrelevant ones (e.g., the table in the last row).

Table 1. Results of point cloud classification on ScanObjectNN dataset. The best, average, and standard deviations of our results in three runs are reported

Method	#point	OA
PointNet [32]	1,024	68.2
PointNet++ [33]	1,024	77.9
DGCNN [44]	1,024	78.1
PointCNN [23]	1,024	78.5
BGA-PN++ [42]	1,024	80.2
BGA-DGCNN [42]	1,024	79.7
SimpleView [12]	1,024	80.5
DynamicScale [35]	1,024	82.0
Ours	1,024	85.8 (85.77±0.06)
MVTN [14]	2,048	82.8
Ours	2,048	87.0 (86.83±0.16)

that increased density provides a better approximation of the underlying surface, thus leading to a significant improvement.

4.3 Part Segmentation

We use 2,048 points with normal information as the input. Random anisotropic scaling and random translation are used for data augmentation. SGD is used for optimization. The initial learning rate is set to 0.1. We use voting for post-processing, as it is a common practice [41,24,50]. The instance-wise average intersection over union (I. mIoU) [33] is used for the performance assessment.

The results are listed in Table 2. The DU-Net achieves competitive performance among cutting-edge models. We believe that DU-Net is especially effective in recognizing object part boundaries, as DUs try to preserve structures while simplifying/smoothing within boundary regions. Although AGCN [19] achieves

Table 2. Results of part segmentation on ShapeNet and scene segmentation on S3DIS (Area 5). The three-run best, average, and standard deviations are reported. Note that we report preprocessing methods for the S3DIS dataset because of their significant impact on the final performance [51,50]

Method	ShapeNet (I. mIoU)	preproc.	S3DIS (mIoU)
PointConv [47]	85.7	-	-
RS-CNN [24]	86.2	-	-
CurveNet [48]	86.8	-	-
AGCN [19]	87.9	-	-
KPConv-rigid [41]	86.2	Grid	65.4
KPConv-d [41]	86.4	Grid	67.1
Point Transformer [56]	86.6	Grid	70.4
PointNet [32]	83.7	BLK	41.1
PointNet++ [33]	85.1	BLK	57.3
PointCNN [23]	86.1	BLK	57.3
PACConv [50]	86.1	BLK	66.6
Ours	87.0 (86.94±0.08)	BLK	66.8(66.72±0.07)



Fig. 8. Qualitative results of part and scene segmentation.

strong performance, it relies on a different training setting and a discriminator network with adversarial training in addition to the segmentation network, which considerably increases the complexity. The qualitative results are shown in Fig. 8.

4.4 Scene Segmentation

Similar to [40], we advocate using Area five for testing and others for training. Following [55], we randomly extract a $1\text{m}\times 1\text{m}$ pillar and take 4,096 points as the input. During the test, we test on all points. We use 3D coordinates, RGB, and normalized 3D coordinates with respect to the maximum coordinates in a room as the inputs. We use SGD with an initial learning rate of 0.1 and train the models for 100 epochs, with each epoch set to 1.5k iterations. Random vertical rotation, random anisotropic scaling, Gaussian jittering, and random color dropout are used for data augmentation. The performance is assessed using the point-average IoU.

The results are reported in Table 2. As mentioned by [51] and [50], the choice of preprocessing methods has a significant impact on the results, which makes comparisons of methods that use different preprocessing procedure difficult. Primarily, we compare our model with other models using the same preprocessing (BLK). We achieve the best performance under the same preprocessing method. The qualitative results are shown in Fig. 8.

5 Design Analysis

Table 3. Results of the ablation study on DU

Model	#DU	ϕ	φ	#neigh.	I. mIoU
A	1			16	85.4
B	1	✓		16	86.3
C	1		✓	16	86.3
D	1	✓	✓	16	86.8
E	2	✓	✓	16	86.7
F	3	✓	✓	16	86.8
G	1	✓	✓	4	86.5
H	1	✓	✓	8	86.6
I	1	✓	✓	24	86.7

Table 4. Incorporating DUs with various convolutions. We take the architecture in Fig.5 as the base model and investigate the performance change by replacing KPConv-l with other convolution methods or unstacking DUs. The reported performance indicate I. mIoU

Convolutions	w/o DU	w/ DU	Δ
PointConv [47]	86.0	86.7	+0.7
RSCConv [24]	86.1	86.4	+0.3
KPConv [41]	86.0	86.3	+0.3
KPConv-l (ours)	86.4	86.8	+0.4

Table 5. Comparison of DU with other edge-aware methods. We take the architecture in Fig.5 as the base model and replace DUs other methods

Method	I. mIoU	#params (M)	Running time (ms)
EdgeConv [44]	85.5	4.0	28.4
Point Trans. [56]	86.5	5.6	27.9
DU	86.8	4.0	26.6

Table 6. Comparison of KPConv and KPConv-l in terms of memory consumption and inference time with different numbers of input points

	Method	10k	20k	40k	80k
Memory (M)	KPConv [41]	1894	2246	3068	4616
	KPConv-l	1608	1844	2288	3096
Inference (ms)	KPConv [41]	94.5	300.5	952.7	3491.9
	KPConv-l	88.4	275.6	922.0	3440.9

In this section, we validate the design choices regarding DU. All experiments are conducted on the ShapeNet (without voting post-processing) because the part segmentation task is sufficiently complex.

DU components. We investigate the influence of DU components. The results are listed in Table 3 (A, B, C, and D). Removing both ϕ and φ leads to significantly degraded performance. Equipping DU with only ϕ or φ achieves acceptable performance (models B and C). The performance reaches a peak when both components are incorporated into DU (model F), which successfully verifies our design choice.

Number of DUs. We investigate the impact of the number of DUs applied to each KPConv-l. As shown in Table 3 (D, E, and F), the performance is not sensitive to the number. Consequently, we set $\#DUs=1$ for all tasks.

Neighborhood size. As listed in Table 3 (D, G, H, and I), the best performance is achieved when $\#neigh$ is selected as 16; therefore, we use 16 as our default choice.

Integrating DU with various convolutions. To show the general applicability of DU, we replace KPConv-l with various popular point convolutions and perform a comparative study. As shown in Table 4, DU successfully boosts other convolution methods, demonstrating its general applicability.

DU vs. other edge-aware methods. We compare DU with EdgeConv [44,22,29] and Point Transformer [56]. For a fair comparison, we replace DUs with other methods in our model. The result is listed in Table 5. Evidently, DU is superior to or on par with other methods in terms of performance, number of parameters, and running time.

KPConv-l vs. KPConv. As shown in Table 6, KPConv-l has a faster inference speed and requires less memory consumption than KPConv. This indicates the usefulness of our trick in the design of KPConv-l.

6 Conclusion

Learning point clouds are difficult due to the lack of connectivity information (i.e., edges). Various edge-aware methods in which constructed edges are used as additional information are proposed, which successfully improve the performance. However, *how* the edges improve the performance is hardly interpretable. In this study, we go beyond edge awareness, and propose the diffusion unit (DU) that performs edge enhancement and suppression adaptively in an interpretable manner. A theoretical analysis is conducted to reveal the underlying mechanism of DU, which is confirmed by the following qualitative analysis using the smoothness information. Concretely, the above analysis reveals that DU learns to enhance task-related edges while suppressing others. Extensive experiments show that the network powered by DUs (DU-Nets) can achieve competitive performance across various challenging benchmarks. In particular, DU-Net achieves the state-of-the-art performance in point cloud classification.

References

1. Armeni, I., Sener, O., Zamir, A.R., Jiang, H., Brilakis, I., Fischer, M., Savarese, S.: 3d semantic parsing of large-scale indoor spaces. In: Proceedings of the IEEE Conference on Computer Vision and Pattern Recognition. pp. 1534–1543 (2016)
2. Atwood, J., Towsley, D.: Diffusion-convolutional neural networks. *Advances in neural information processing systems* **29** (2016)
3. Bajaj, C.L., Xu, G.: Anisotropic diffusion of surfaces and functions on surfaces. *ACM Transactions on Graphics (TOG)* **22**(1), 4–32 (2003)
4. Black, M.J., Sapiro, G., Marimont, D.H., Heeger, D.: Robust anisotropic diffusion. *IEEE Transactions on image processing* **7**(3), 421–432 (1998)
5. Brox, T., Weickert, J., Burgeth, B., Mrázek, P.: Nonlinear structure tensors. *Image and Vision Computing* **24**(1), 41–55 (2006)
6. Chamberlain, B., Rowbottom, J., Gorinova, M.I., Bronstein, M., Webb, S., Rossi, E.: Grand: Graph neural diffusion. In: International Conference on Machine Learning. pp. 1407–1418. PMLR (2021)
7. Choy, C., Gwak, J., Savarese, S.: 4d spatio-temporal convnets: Minkowski convolutional neural networks. In: Proceedings of the IEEE/CVF Conference on Computer Vision and Pattern Recognition. pp. 3075–3084 (2019)
8. Clarenz, U., Diewald, U., Rumpf, M.: Anisotropic geometric diffusion in surface processing. *IEEE* (2000)
9. Cui, Y., Chen, R., Chu, W., Chen, L., Tian, D., Li, Y., Cao, D.: Deep learning for image and point cloud fusion in autonomous driving: A review. *IEEE Transactions on Intelligent Transportation Systems* (2021)
10. Desbrun, M., Meyer, M., Schröder, P., Barr, A.H.: Implicit fairing of irregular meshes using diffusion and curvature flow. In: Proceedings of the 26th annual conference on Computer graphics and interactive techniques. pp. 317–324 (1999)
11. Feng, Y., Zhang, Z., Zhao, X., Ji, R., Gao, Y.: Gvcnn: Group-view convolutional neural networks for 3d shape recognition. In: Proceedings of the IEEE Conference on Computer Vision and Pattern Recognition. pp. 264–272 (2018)
12. Goyal, A., Law, H., Liu, B., Newell, A., Deng, J.: Revisiting point cloud shape classification with a simple and effective baseline. *International Conference on Machine Learning* (2021)
13. Graham, B., Engelcke, M., Van Der Maaten, L.: 3d semantic segmentation with submanifold sparse convolutional networks. In: Proceedings of the IEEE conference on computer vision and pattern recognition. pp. 9224–9232 (2018)
14. Hamdi, A., Giancola, S., Ghanem, B.: Mvtn: Multi-view transformation network for 3d shape recognition. In: Proceedings of the IEEE/CVF International Conference on Computer Vision. pp. 1–11 (2021)
15. Howard, A.G., Zhu, M., Chen, B., Kalenichenko, D., Wang, W., Weyand, T., Andreetto, M., Adam, H.: Mobilenets: Efficient convolutional neural networks for mobile vision applications. *arXiv preprint arXiv:1704.04861* (2017)
16. Hu, Z., Zhen, M., Bai, X., Fu, H., Tai, C.I.: Jsenet: Joint semantic segmentation and edge detection network for 3d point clouds. In: European Conference on Computer Vision. pp. 222–239. Springer (2020)
17. Jiang, L., Zhao, H., Liu, S., Shen, X., Fu, C.W., Jia, J.: Hierarchical point-edge interaction network for point cloud semantic segmentation. In: Proceedings of the IEEE/CVF International Conference on Computer Vision. pp. 10433–10441 (2019)

18. Kanezaki, A., Matsushita, Y., Nishida, Y.: Rotationnet: Joint object categorization and pose estimation using multiviews from unsupervised viewpoints. In: Proceedings of the IEEE Conference on Computer Vision and Pattern Recognition. pp. 5010–5019 (2018)
19. Kim, S., Alexander, D.C.: Agcn: Adversarial graph convolutional network for 3d point cloud segmentation (2021)
20. Kingma, D.P., Ba, J.: Adam: A method for stochastic optimization. In: ICLR (Poster) (2015)
21. Lan, S., Yu, R., Yu, G., Davis, L.S.: Modeling local geometric structure of 3d point clouds using geo-cnn. In: Proceedings of the IEEE/CVF Conference on Computer Vision and Pattern Recognition. pp. 998–1008 (2019)
22. Li, G., Muller, M., Thabet, A., Ghanem, B.: Deepgcn: Can gcn go as deep as cnns? In: Proceedings of the IEEE/CVF international conference on computer vision. pp. 9267–9276 (2019)
23. Li, Y., Bu, R., Sun, M., Wu, W., Di, X., Chen, B.: Pointcnn: Convolution on χ -transformed points. In: Proceedings of the 32nd International Conference on Neural Information Processing Systems. pp. 828–838 (2018)
24. Liu, Y., Fan, B., Xiang, S., Pan, C.: Relation-shape convolutional neural network for point cloud analysis. In: Proceedings of the IEEE/CVF Conference on Computer Vision and Pattern Recognition. pp. 8895–8904 (2019)
25. Liu, Z., Hu, H., Cao, Y., Zhang, Z., Tong, X.: A closer look at local aggregation operators in point cloud analysis. In: European Conference on Computer Vision. pp. 326–342. Springer (2020)
26. Luo, S., Hu, W.: Diffusion probabilistic models for 3d point cloud generation. In: Proceedings of the IEEE/CVF Conference on Computer Vision and Pattern Recognition. pp. 2837–2845 (2021)
27. Mao, J., Wang, X., Li, H.: Interpolated convolutional networks for 3d point cloud understanding. In: Proceedings of the IEEE/CVF International Conference on Computer Vision. pp. 1578–1587 (2019)
28. Maturana, D., Scherer, S.: Voxnet: A 3d convolutional neural network for real-time object recognition. In: 2015 IEEE/RSJ International Conference on Intelligent Robots and Systems (IROS). pp. 922–928. IEEE (2015)
29. Pan, L.: Ecg: Edge-aware point cloud completion with graph convolution. IEEE Robotics and Automation Letters **5**(3), 4392–4398 (2020)
30. Perona, P., Malik, J.: Scale-space and edge detection using anisotropic diffusion. IEEE Transactions on pattern analysis and machine intelligence **12**(7), 629–639 (1990)
31. Qi, C.R., Liu, W., Wu, C., Su, H., Guibas, L.J.: Frustum pointnets for 3d object detection from rgb-d data. In: Proceedings of the IEEE conference on computer vision and pattern recognition. pp. 918–927 (2018)
32. Qi, C.R., Su, H., Mo, K., Guibas, L.J.: Pointnet: Deep learning on point sets for 3d classification and segmentation. In: Proceedings of the IEEE conference on computer vision and pattern recognition. pp. 652–660 (2017)
33. Qi, C.R., Yi, L., Su, H., Guibas, L.J.: Pointnet++: Deep hierarchical feature learning on point sets in a metric space. Advances in Neural Information Processing Systems **30** (2017)
34. Ronneberger, O., Fischer, P., Brox, T.: U-net: Convolutional networks for biomedical image segmentation. In: International Conference on Medical image computing and computer-assisted intervention. pp. 234–241. Springer (2015)

35. Sheshappanavar, S.V., Kambhamettu, C.: Dynamic local geometry capture in 3d point cloud classification. In: 2021 IEEE 4th International Conference on Multimedia Information Processing and Retrieval (MIPR). pp. 158–164. IEEE (2021)
36. Shinohara, T., Xiu, H., Matsuoka, M.: Fwnet: Semantic segmentation for full-waveform lidar data using deep learning. *Sensors* **20**(12), 3568 (2020)
37. Sifre, L., Mallat, S.: Rigid-motion scattering for texture classification. arXiv preprint arXiv:1403.1687 (2014)
38. Simonovsky, M., Komodakis, N.: Dynamic edge-conditioned filters in convolutional neural networks on graphs. In: Proceedings of the IEEE conference on computer vision and pattern recognition. pp. 3693–3702 (2017)
39. Su, H., Maji, S., Kalogerakis, E., Learned-Miller, E.: Multi-view convolutional neural networks for 3d shape recognition. In: Proceedings of the IEEE international conference on computer vision. pp. 945–953 (2015)
40. Tchapmi, L., Choy, C., Armeni, I., Gwak, J., Savarese, S.: Segcloud: Semantic segmentation of 3d point clouds. In: 2017 international conference on 3D vision (3DV). pp. 537–547. IEEE (2017)
41. Thomas, H., Qi, C.R., Deschaud, J.E., Marcotegui, B., Goulette, F., Guibas, L.J.: Kpconv: Flexible and deformable convolution for point clouds. In: Proceedings of the IEEE/CVF International Conference on Computer Vision. pp. 6411–6420 (2019)
42. Uy, M.A., Pham, Q.H., Hua, B.S., Nguyen, T., Yeung, S.K.: Revisiting point cloud classification: A new benchmark dataset and classification model on real-world data. In: Proceedings of the IEEE/CVF International Conference on Computer Vision. pp. 1588–1597 (2019)
43. Wang, L., Huang, Y., Hou, Y., Zhang, S., Shan, J.: Graph attention convolution for point cloud semantic segmentation. In: Proceedings of the IEEE/CVF Conference on Computer Vision and Pattern Recognition. pp. 10296–10305 (2019)
44. Wang, Y., Sun, Y., Liu, Z., Sarma, S.E., Bronstein, M.M., Solomon, J.M.: Dynamic graph cnn for learning on point clouds. *Acm Transactions On Graphics (tog)* **38**(5), 1–12 (2019)
45. Weickert, J.: Anisotropic diffusion in image processing, vol. 1. Teubner Stuttgart (1998)
46. Weickert, J.: Coherence-enhancing diffusion filtering. *International journal of computer vision* **31**(2), 111–127 (1999)
47. Wu, W., Qi, Z., Fuxin, L.: Pointconv: Deep convolutional networks on 3d point clouds. In: Proceedings of the IEEE/CVF Conference on Computer Vision and Pattern Recognition. pp. 9621–9630 (2019)
48. Xiang, T., Zhang, C., Song, Y., Yu, J., Cai, W.: Walk in the cloud: Learning curves for point clouds shape analysis. In: Proceedings of the IEEE/CVF International Conference on Computer Vision (ICCV) (October 2021)
49. Xiu, H., Liu, X., Wang, W., Kim, K.S., Shinohara, T., Chang, Q., Matsuoka, M.: Enhancing local feature learning for 3d point cloud processing using unary-pairwise attention. arXiv preprint arXiv:2203.00172 (2022)
50. Xu, M., Ding, R., Zhao, H., Qi, X.: Paconv: Position adaptive convolution with dynamic kernel assembling on point clouds. arXiv preprint arXiv:2103.14635 (2021)
51. Yan, X., Zheng, C., Li, Z., Wang, S., Cui, S.: Pointasnl: Robust point clouds processing using nonlocal neural networks with adaptive sampling. In: Proceedings of the IEEE/CVF Conference on Computer Vision and Pattern Recognition. pp. 5589–5598 (2020)

52. Yi, L., Kim, V.G., Ceylan, D., Shen, I.C., Yan, M., Su, H., Lu, C., Huang, Q., Sheffer, A., Guibas, L.: A scalable active framework for region annotation in 3d shape collections. *ACM Transactions on Graphics (ToG)* **35**(6), 1–12 (2016)
53. Yu, L., Li, X., Fu, C.W., Cohen-Or, D., Heng, P.A.: Ec-net: an edge-aware point set consolidation network. In: *Proceedings of the European conference on computer vision (ECCV)*. pp. 386–402 (2018)
54. Zhang, Z., Hua, B.S., Yeung, S.K.: Shellnet: Efficient point cloud convolutional neural networks using concentric shells statistics. In: *Proceedings of the IEEE/CVF International Conference on Computer Vision*. pp. 1607–1616 (2019)
55. Zhao, H., Jiang, L., Fu, C.W., Jia, J.: Pointweb: Enhancing local neighborhood features for point cloud processing. In: *Proceedings of the IEEE/CVF Conference on Computer Vision and Pattern Recognition*. pp. 5565–5573 (2019)
56. Zhao, H., Jiang, L., Jia, J., Torr, P., Koltun, V.: Point transformer. In: *ICCV* (2021)
57. Zhao, J., Dong, Y., Ding, M., Kharlamov, E., Tang, J.: Adaptive diffusion in graph neural networks. *Advances in Neural Information Processing Systems* **34** (2021)
58. Zhou, Y., Tuzel, O.: Voxelnet: End-to-end learning for point cloud based 3d object detection. In: *Proceedings of the IEEE Conference on Computer Vision and Pattern Recognition*. pp. 4490–4499 (2018)
59. Zhu, X.X., Tuia, D., Mou, L., Xia, G.S., Zhang, L., Xu, F., Fraundorfer, F.: Deep learning in remote sensing: A comprehensive review and list of resources. *IEEE Geoscience and Remote Sensing Magazine* **5**(4), 8–36 (2017)